EURASIP Journal on Wireless Communications and Networking 2005:3, 364–381

Flexible Analog Front Ends of Reconfigurable Radios Based on Sampling and Reconstruction with Internal Filtering

Yefim S. Poberezhskiy
Rockwell Scientific Company, Thousand Oaks, CA 91360, USA
Email: ypoberezhskiy@rwsc.com

Gennady Y. Poberezhskiy
Raytheon Company, El Segundo, CA 90245, USA
Email: gennady@raytheon.com

Received 27 September 2004; Revised 4 April 2005

Bandpass sampling, reconstruction, and antialiasing filtering in analog front ends potentially provide the best performance of software defined radios. However, conventional techniques used for these procedures limit reconfigurability and adaptivity of the radios, complicate integrated circuit implementation, and preclude achieving potential performance. Novel sampling and reconstruction techniques with internal filtering eliminate these drawbacks and provide many additional advantages. Several ways to overcome the challenges of practical realization and implementation of these techniques are proposed and analyzed. The impact of sampling and reconstruction with internal filtering on the analog front end architectures and capabilities of software defined radios is discussed.

Keywords and phrases: software defined radios, reconfigurable and adaptive transceivers, sampling, analog signal reconstruction, antialiasing filtering, A/D.

1. INTRODUCTION

Next generation of software defined radios (SDRs) should be reconfigurable to support future wireless systems operating with different existing and evolving communication standards while providing a wide variety of services over various networks. These SDRs should also be extremely adaptive to achieve high performance in dynamic communication environment and to accommodate varying user needs. Modern radios, virtually all of which are digital, do not meet these requirements. They contain large analog front ends, that is, their analog and mixed-signal portions (AMPs) [1, 2, 3, 4, 5, 6, 7, 8, 9, 10, 11, 12, 13, 14, 15, 16]. The AMPs are much less flexible and have much lower scale of integration than the radios' digital portions (DPs). The AMPs are also sources of many types of interference and signal distortion. It can be stated that reconfigurability, adaptivity, performance, and scale of integration of modern SDRs are limited by their AMPs. Therefore, only radical changes in the design of the AMPs allow development of really reconfigurable SDRs.

It is shown in this paper that the changes in the AMP design have to be related first of all to the methods of sampling, reconstruction, and antialiasing filtering. It is also shown that implementation of novel sampling and reconstruction techniques with internal filtering [17, 18, 19, 20, 21, 22, 23] will make the AMPs of SDRs almost as flexible as their DPs and significantly improve performance of SDRs. To this end, conventional architectures of the radio AMPs are briefly examined in Section 2. It is shown that the architectures that potentially can provide the best performance have the lowest flexibility and scale of integration. The main causes of the conventional architectures' drawbacks are determined. In Section 3, novel sampling and reconstruction techniques with internal filtering are described. The sampling technique was obtained as a logical step in the development of integrating sample-and-hold amplifiers (SHAs) in [17, 18]. In [19, 20], it was derived from the sampling theorem. The reconstruction technique with internal filtering was derived from the sampling theorem in [21]. Initial analysis of both techniques was performed in [22, 23]. Section 3 contains examination of their features and capabilities, which is more detailed than that in [22, 23]. Challenges of these techniques' implementation and two methods of modification of sampling circuits (SCs) with internal antialiasing filtering are

analyzed in Section 4. Since SCs and reconstruction circuits (RCs) with internal filtering are inherently multichannel, mitigation of the channel mismatch impact on the performance of the SDRs is discussed in Section 5. Architectures of the AMPs modified to accommodate sampling and reconstruction with internal filtering are considered in Section 6.

2. CONVENTIONAL ARCHITECTURES OF THE RADIO AMPS

2.1. AMPs of receivers

In digital receivers, the main purpose of AMPs is to create conditions for signal digitization. Indeed, AMPs, regardless of their architectures, carry out the following main functions: antialiasing filtering, amplification of received signals to the level required for the analog-to-digital converter (A/D), and conversion of the signals to the frequency most convenient for sampling and quantization. Besides, they often provide band selection, image rejection, and some other types of frequency selection to lower requirements for the dynamic range of subsequent circuits. Most AMPs of modern receivers belong to one of three basic architectures: direct conversion architecture, superheterodyne architecture with baseband sampling, and superheterodyne architecture with bandpass sampling. The examples of these architectures are shown in Figure 1.

In a direct conversion (homodyne) architecture (see Figure 1a), a radio frequency (RF) section performs preliminary filtering and amplification of the sum of a desired signal, noise, and interference. Then, this sum is converted to the baseband, forming its in-phase (I) and quadrature (Q) components. A local oscillator (LO), which generates sine and cosine components at radio frequency f_r, is tunable within the receiver frequency range. Lowpass filters (LPFs) provide antialiasing filtering of the I and Q components while SHAs and A/Ds carry out their sampling and quantization. Channel filtering is performed digitally in the receiver DP. For simplicity, circuits providing frequency tuning, gain control, and other auxiliary functions are not shown in Figure 1 and subsequent figures. Although integrated circuit (IC) implementation of this architecture encounters many difficulties, it is simpler than that of the architectures shown in Figures 1b and 1c.

In a superheterodyne architecture with baseband sampling (see Figure 1b), the sum of a desired signal, noise, and interference is converted to intermediate frequency (IF) f_0 after image rejection and preliminary amplification in the RF section. Antialiasing filtering is performed at a fixed IF. This enables the use of bandpass filters with high selectivity, for example, surface acoustic wave (SAW), crystal, mechanical, and ceramic. Then, the sum is converted to the baseband and its I and Q components are formed.

An example of a superheterodyne architecture with bandpass sampling is shown in Figure 1c. In most cases, such receivers have two frequency conversions. The 1st IF is usually selected high enough to simplify image rejection and reduce the number of spurious responses. The 2nd IF is typically chosen to simplify antialiasing filtering and digitization. Double frequency conversion also allows division of the AMP gain between the 1st and 2nd IF strips. This architecture performs real-valued bandpass sampling, representing signals by the samples of their instantaneous values. In the DP, these samples are converted to the samples of I and Q components (complex-valued representation), to make digital signal processing more efficient.

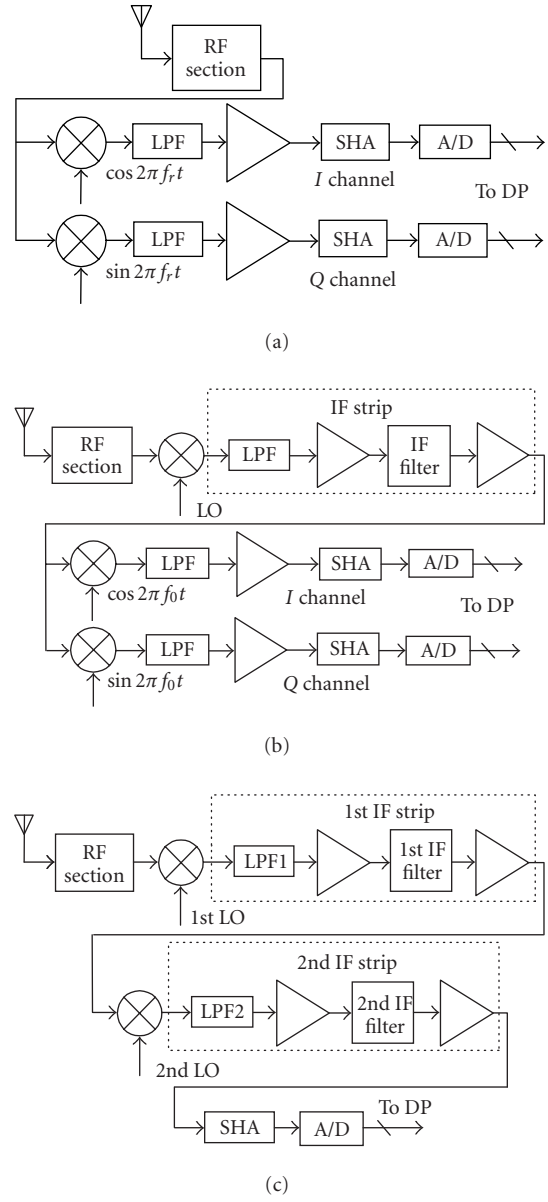

Figure 1: Receiver AMP architectures: (a) direct conversion architecture, (b) superheterodyne architecture with baseband sampling, and (c) superheterodyne architecture with bandpass sampling.

The results of comparative analysis of the described architectures are reflected in Table 1. This analysis is not detailed because each basic architecture has many modifications. For example, superheterodyne architectures may have

Table 1: Comparison of various AMP architectures of modern receivers.

Architecture	Advantages	Drawbacks
Direct conversion receiver architecture	Absence of spectral images caused by frequency conversion	Significant phase and amplitude imbalances between I and Q channels
	Better adaptivity compared to other modern architectures	High nonlinear distortions due to the fall of substantial part of IMPs within the signal spectrum
	Better compatibility of AMP technology with IC technology compared to other architectures	LO leakage that creates interference to other receivers and contributes to the DC offset
	Relatively low requirements for SHA and A/D	Relatively low selectivity of antialiasing filtering
	Minimum cost, size, and weight	Direct current (DC) offset caused by many factors
		Flicker noise
Superheterodyne receiver architecture with baseband sampling	Radical reduction of LO leakage due to the offset frequency conversion	High nonlinear distortions due to the fall of substantial part of IMPs within signal spectrum
	High selectivity of antialiasing filtering provided by SAW, crystal, mechanical, or ceramic IF filters	Low adaptivity and reconfigurability of the receiver AMP due to the use of SAW, crystal, mechanical, or ceramic IF filters
	Slight reduction of phase and amplitude imbalances between I and Q channels compared to the direct conversion architecture (due to conversion from a constant IF to zero frequency)	Incompatibility of AMP technology with IC technology due to the use of SAW, crystal, mechanical, or ceramic IF filters
	Reduction of flicker noise due to lesser gain at zero frequency	Still significant phase and amplitude imbalances between I and Q channels
	Relatively low requirements for SHA and A/D	Spurious responses due to frequency conversions
		Still significant flicker noise
Superheterodyne receiver architecture with bandpass sampling	Radical reduction of LO leakage due to offset frequency conversion	Low adaptivity and reconfigurability of the receiver AMP due to the use of SAW, crystal, mechanical, or ceramic IF filters
	High selectivity of antialiasing filtering provided by SAW, crystal, mechanical, or ceramic IF filters	Incompatibility of AMP technology with IC technology due to the use of SAW, crystal, mechanical, or ceramic IF filters
	Exclusion of phase and amplitude imbalances between I and Q channels	Still high nonlinear distortions due to large input current of SHA
	Exclusion of DC offset and flicker noise	Spurious responses due to frequency conversions
	Minimum IMPs falling within the signal spectrum	Highest requirements for SHA and A/D

different number of frequency conversions, and even the architectures with a single conversion have different properties depending on the parameters of their IF strips. For instance, selection of a low IF in a single-conversion architecture enables replacement of high-selectivity off-chip IF filters with active filters. This increases flexibility and scale of integration of an AMP at the expense of more complicated image rejection.

Despite the absence of some details, Table 1 conclusively shows that the superheterodyne architecture with bandpass sampling has advantages that cannot be provided by other architectures. Indeed, only bandpass sampling minimizes the number of intermodulation products (IMPs) falling within the signal spectrum. It also excludes phase and amplitude imbalances between I and Q channels, DC offset, and flicker noise. The drawbacks of this architecture have the following causes. Low adaptivity, reconfigurability, and scale of integration of the AMPs are caused by inflexibility of the best IF filters (e.g., SAW, crystal, mechanical, and ceramic) and incompatibility of their technology with IC technology. Inflexibility of these filters also does not allow avoiding spurious responses. Two times higher sampling frequency required for bandpass sampling raises requirements for SHA and A/D. At present, track-and-hold amplifiers (THAs) are usually used

as SHAs for bandpass sampling. A THA does not suppress out-of-band noise and IMPs of all the stages between the antialiasing filter and the THA capacitor. As a result of sampling, these noise and IMPs fall within the signal spectrum. The impact of this phenomenon is especially significant in receivers with bandpass sampling. THAs need large input current because they utilize only a small fraction of signal energy for sampling. The large input current requires a significant AMP gain. This makes sampling close to the antenna impossible. The large input current also increases nonlinear distortions. Higher frequency of bandpass signals compared to baseband ones further increases the required THA input current and, consequently, nonlinear distortions. THAs are very susceptible to jitter.

It is important to add that conventional sampling procedures have no theoretical basis. In contrast, sampling with internal antialiasing filtering has been derived from the sampling theorem. As shown in Section 3, it eliminates the drawbacks of conventional sampling.

2.2. AMPs of transmitters

An AMP of a digital transmitter, regardless of its architecture, has to perform reconstruction filtering, conversion of reconstructed signals to the RF, and their amplification. Similar to the receivers, modern transmitters have three basic AMP architectures: direct up-conversion architecture, offset up-conversion architecture with baseband reconstruction, and offset up-conversion architecture with bandpass reconstruction. Simplified block diagrams of these architectures are shown in Figure 2.

In a direct up-conversion architecture (see Figure 2a), modulation and channel filtering are carried out in the transmitter DP using complex-valued representation. The I and Q outputs of the DP are converted to analog samples by D/As. After baseband filtering and amplification of I and Q components, an analog bandpass signal is formed directly at the transmitter RF. An LO, which generates $\cos 2\pi f_r t$ and $\sin 2\pi f_r t$, is tunable within the transmitter frequency range. The formed RF signal passes through a bandpass filter (BPF) that filters out unwanted products of frequency up-conversion, and enters a power amplifier (PA). This architecture is the most flexible and suitable for IC implementation among modern architectures. However, it cannot provide high performance. The baseband reconstruction causes significant amplitude and phase imbalances between the I and Q channels, DC offset, and nonlinear distortions that reduce the accuracy of modulation. The DC offset also causes the LO leakage through the antenna. Additional problem of this architecture is that a voltage-controlled oscillator (VCO), used as an LO, is sensitive to pulling from the PA output.

An AMP architecture with offset up-conversion and baseband reconstruction (see Figure 2b) is not susceptible to VCO pulling. It provides better reconstruction filtering than the previous architecture due to the use of SAW, crystal, mechanical, or ceramic IF filters and allows slightly more accurate formation of bandpass signals since it is performed at a constant IF. If the IF is selected higher than the upper bound

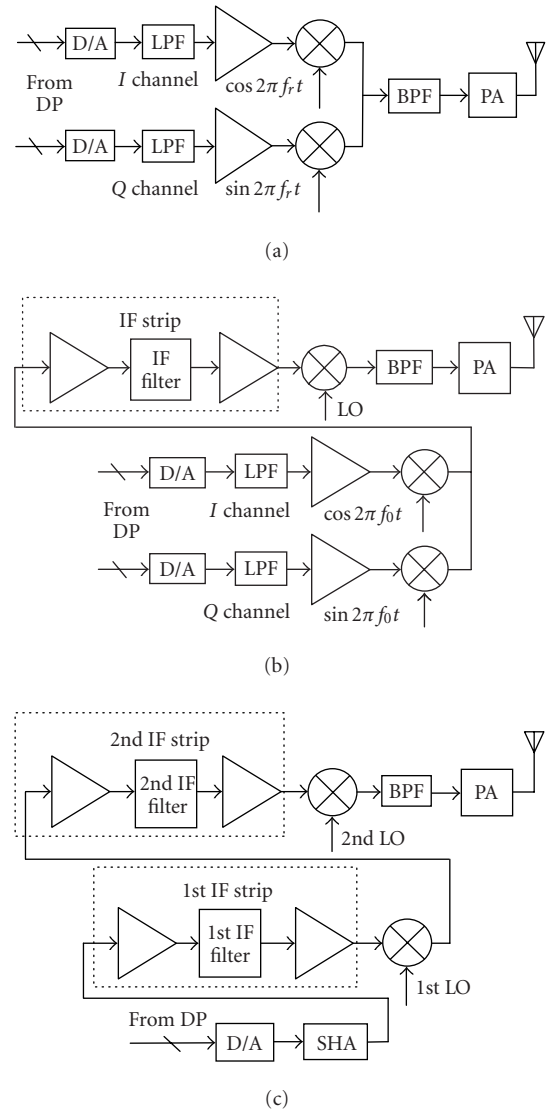

Figure 2: Transmitter AMP architectures: (a) direct up-conversion architecture, (b) offset up-conversion architecture with baseband reconstruction, (c) offset up-conversion architecture with bandpass reconstruction.

of the transmitter RF band, the BPF in the AMP can be replaced by an LPF. This architecture still has all the drawbacks related to baseband reconstruction.

These drawbacks are eliminated in an offset up-conversion architecture with bandpass reconstruction shown in Figure 2c. Here, a bandpass IF signal is formed digitally in the DP. This reduces nonlinear distortions and excludes DC offset and amplitude and phase imbalances between I and Q channels. As a result, modulation becomes more accurate, and a spurious carrier is not present. However, like in the case of receivers, these advantages are achieved at the expense of reduced adaptivity of the AMP and incompatibility of its technology with IC technology caused by the most effective IF reconstruction filters. Besides, the sample mode

Table 2: Comparison of various AMP architectures of modern transmitters.

Architecture	Advantages	Drawbacks
Direct up-conversion transmitter architecture	Better compatibility of AMP technology with IC technology compared to other modern architectures	Low accuracy of modulation due to significant phase and amplitude imbalances between I and Q channels, DC offset, and nonlinear distortions
	Better adaptivity compared to other modern architectures	LO leakage through the antenna caused by DC offset and other factors
		Pulling voltage-controlled LO from PA output
Offset up-conversion transmitter architecture with baseband reconstruction	Insusceptibility to pulling the voltage-controlled LO from the PA output	Low accuracy of modulation due to significant phase and amplitude imbalances between I and Q channels, DC offset, and nonlinear distortion
	High selectivity of reconstruction filtering due to the use of SAW, crystal, mechanical, or ceramic IF filters	Low adaptivity and reconfigurability of AMP due to the use of SAW, crystal, mechanical, or ceramic IF filters
	Slightly better accuracy of modulation due to forming a bandpass signal at a constant IF	Incompatibility of AMP technology with IC technology due to the use of SAW, crystal, mechanical, or ceramic IF filters
	Reduction of LO leakage	
Offset up-conversion transmitter architecture with bandpass reconstruction	The highest accuracy of modulation due to radical reduction of phase and amplitude imbalances between I and Q channels, DC offset, and nonlinear distortion	Low adaptivity and reconfigurability of AMP due to the use of SAW, crystal, mechanical, or ceramic filters
	Insusceptibility to pulling voltage-controlled LO from PA output	Incompatibility of AMP technology with IC technology due to the use of SAW, crystal, mechanical, or ceramic filters
	High selectivity of reconstruction filtering due to the use of SAW, crystal, mechanical, or ceramic filters	Incomplete utilization of D/A output power
	Radical reduction of LO leakage	High requirements for D/A

length Δt_s in a conventional SHA at the D/A output should meet the condition

$$\Delta t_s \leq \frac{1}{(2f_0)}, \tag{1}$$

where f_0 is a center frequency of the reconstructed signal, which coincides with the 1st IF. Condition (1) can be bypassed by using SHA with weighted integration. However, they are not used. Condition (1) does not allow efficient utilization of the D/A output current and, consequently, signal reconstruction close to the antenna.

The results of the comparative analysis of the described transmitter AMP architectures are reflected in Table 2. Since each basic architecture has many modifications, this analysis is not detailed. However, it shows that the offset up-conversion architecture with bandpass reconstruction provides the highest accuracy of modulation. As to the drawbacks of this architecture, they can be eliminated by implementation of the proposed reconstruction technique with internal filtering (see Section 3).

3. SAMPLING AND RECONSTRUCTION WITH INTERNAL FILTERING

3.1. General

As shown in Section 2, AMPs with bandpass sampling, reconstruction, and filtering provide the best performance of both receivers and transmitters (see Figures 1c and 2c). At the same time, conventional methods of sampling, reconstruction, and filtering limit flexibility of the AMPs, complicate their IC implementation, and prevent achieving potential performance. Novel sampling and reconstruction techniques with internal filtering [17, 18, 19, 20, 21, 22, 23] allow elimination of these drawbacks and provide additional benefits. These techniques have a strong theoretical foundation because they are derived from the sampling theorem. They can be used for both bandpass and baseband sampling and reconstruction. However, this paper is mainly focused on bandpass applications of the proposed techniques since the techniques are more beneficial for these applications.

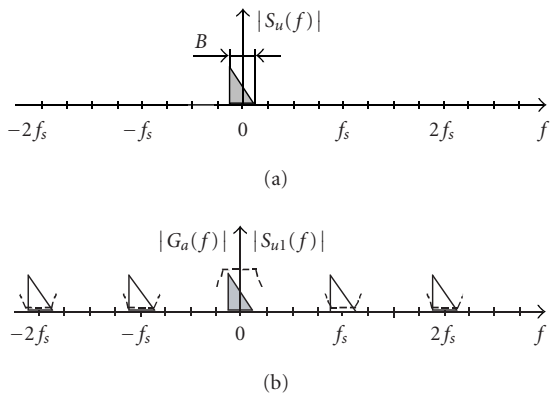

Figure 3: Amplitude spectra and the desired AFR: (a) $|S_u(f)|$, (b) $|S_{u1}(f)|$ and $|G_a(f)|$ (dashed line).

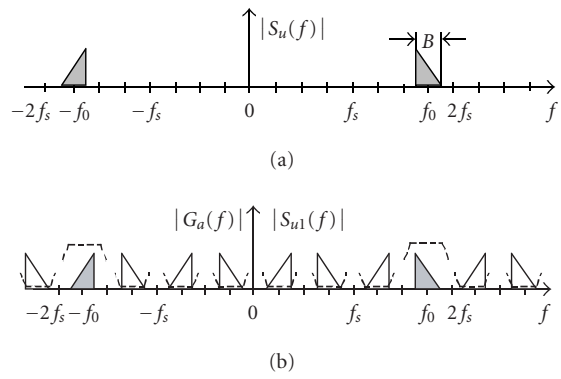

Figure 4: Amplitude spectra and the desired AFR: (a) $|S_u(f)|$, (b) $|S_{u1}(f)|$ and $|G_a(f)|$ (dashed line).

3.2. Antialiasing and reconstruction filtering

To better describe operation of sampling and reconstruction circuits (SCs and RCs) with internal filtering, we first specify requirements for antialiasing and reconstruction filtering. An antialiasing filter should minimally distort analog signal $u(t)$ intended for sampling and maximally suppress noise and interference that can fall within the signal spectrum $S_u(f)$ as a result of sampling.

When baseband sampling takes place, spectrum $S_u(f)$ of a complex-valued $u(t)$, represented by its $I$and Q components, occupies the interval (see Figure 3a)

$$[-0.5B, +0.5B], \tag{2}$$

where B is a bandwidth of $u(t)$. Sampling with frequency f_s causes replication of $S_u(f)$ with period f_s (see Figure 3b) and mapping the whole f-axis for $u(t)$ into the region $[-0.5f_s, 0.5f_s[$ for the sampled signal $u(nT_s)$, where $T_s = 1/f_s$ is a sampling period. Thus, antialiasing filter should cause minimum distortion within interval (2) and suppress noise and interference within the intervals

$$[kf_s - 0.5B, kf_s + 0.5B], \tag{3}$$

where replicas of $S_u(f)$ are located in the spectrum $S_{u1}(f)$ of $u(nT_s)$. In (3), k is any nonzero integer. In principle, noise and interference within the gaps between all intervals (3) and (2) can be suppressed in the DP. However, if these noise and interference are comparable with or greater than $u(t)$, weakening them by an SC lowers requirements for the resolution of an A/D and DP. A desired amplitude-frequency response (AFR) $|G_a(f)|$ of an antialiasing filter is shown in Figure 3b by the dashed line.

In the case of reconstruction, it is necessary to suppress all the images of $u(nT_s)$ within intervals (3) and minimally distort the image within interval (2). No suppression within the gaps between intervals (3) and (2) is usually required.

When bandpass sampling takes place, spectrum $S_u(f)$ of real-valued bandpass $u(t)$ occupies the intervals

$$[-f_0 - 0.5B, -f_0 + 0.5B] \cup [f_0 - 0.5B, f_0 + 0.5B], \tag{4}$$

where f_0 is a center frequency of $S_u(f)$. A plot of $S_u(f)$ is shown in Figure 4a. For bandpass sampling and reconstruction, f_s usually meets the condition

$$f_s = \frac{f_0}{\{\text{floor}\,[(f_0/f_s) + 0.5] \pm 0.25\}}. \tag{5}$$

Selection of f_s according to (5) minimizes aliasing and simplifies both digital forming of I and Q components at the output of the receiver A/D and digital forming of a bandpass signal at the input of the transmitter D/A. Therefore, f_s that meets (5) is considered optimal. When f_s is optimal, an antialiasing filter should cause minimum distortion within intervals (4) and suppress noise and interference within the intervals

$$\begin{aligned}&[-(f_0 + 0.5B + 0.5rf_s), -(f_0 - 0.5B + 0.5rf_s)]\\ &\cup [f_0 - 0.5B + 0.5rf_s, f_0 + 0.5B + 0.5rf_s],\end{aligned} \tag{6}$$

where r is an integer, $r \in [(0.5 - 2f_0/f_s), \infty[$, $r \neq 0$. Figure 4b shows amplitude spectrum $|S_{u1}(f)|$ of $u(nT_s)$, and the desired AFR $|G_a(f)|$ of an antialiasing filter for bandpass sampling. Thus, a bandpass antialiasing filter has to suppress noise and interference within intervals (6) and minimally distort $u(t)$ within intervals (4). Suppression of noise and interference within the gaps between intervals (4) and (6) is not mandatory, but it can be used to lower requirements for the resolution of an A/D and DP.

Bandpass reconstruction requires only suppression of $u(nT_s)$ images within intervals (6) and minimum distortion within intervals (4).

3.3. Canonical sampling circuits

The block diagrams of two canonical SCs with internal antialiasing filtering are shown in Figure 5. In Figure 5a, an input signal $u_i(t)$ is fed into L parallel channels, whose outputs are in turn connected to an A/D by a multiplexer (Mx). The spectrum of $u_i(t)$ is not limited by an antialiasing filter and includes the spectrum of the signal $u(t)$ that should be sampled. The lth channel ($l \in [1, L]$) forms all samples with

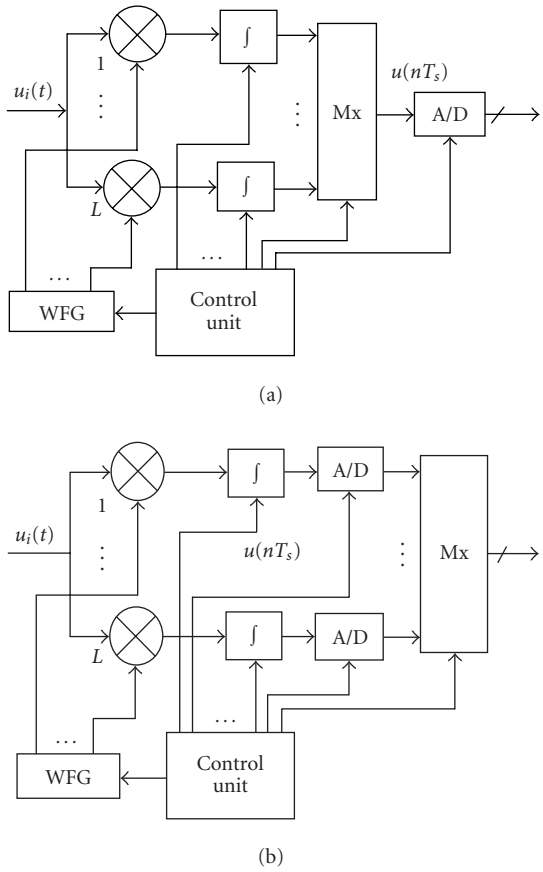

Figure 5: Canonical SCs with internal antialiasing filtering: (a) single-A/D version and (b) multiple-A/D version.

numbers $l + kL$, where k is any integer. The operational cycle of each channel is equal to LT_s, consists of three modes (sample, hold, and clear), and is shifted by T_s relative to the operational cycle of the previous channel. The length of the sample mode is equal to T_w, where T_w is the length of weight function $w_0(t)$.

During the sample mode, $u_i(t)$ is multiplied by $w_n(t) = w_0(t - nT_s)$, and the product is integrated. As a result,

$$u(nT_s) = \int_{nT_s - 0.5T_w}^{nT_s + 0.5T_w} u_i(\tau) \cdot w_n(\tau) \cdot d\tau. \tag{7}$$

Equation (7) reflects sampling, accumulation of the signal energy with weight $w_0(t)$, and antialiasing filtering with impulse response $h(t) = w_0(nT_s + 0.5T_w - t)$. Throughout the hold mode with length T_h, a channel is connected to the A/D that quantizes the channel output. In the clear mode with length T_c, the channel is disconnected from the A/D, and the capacitor of its integrator is discharged. It is reasonable to allocate T_s for both hold and clear modes: $T_h + T_c = T_s$. A weight function generator (WFG) simultaneously generates $L-1$ copies $w_n(t)$ of $w_0(t)$ because, at any instant, $L-1$ channels are in the sample mode, and one channel is in the hold or clear mode. Each $w_n(t)$ is shifted relative to the previous one

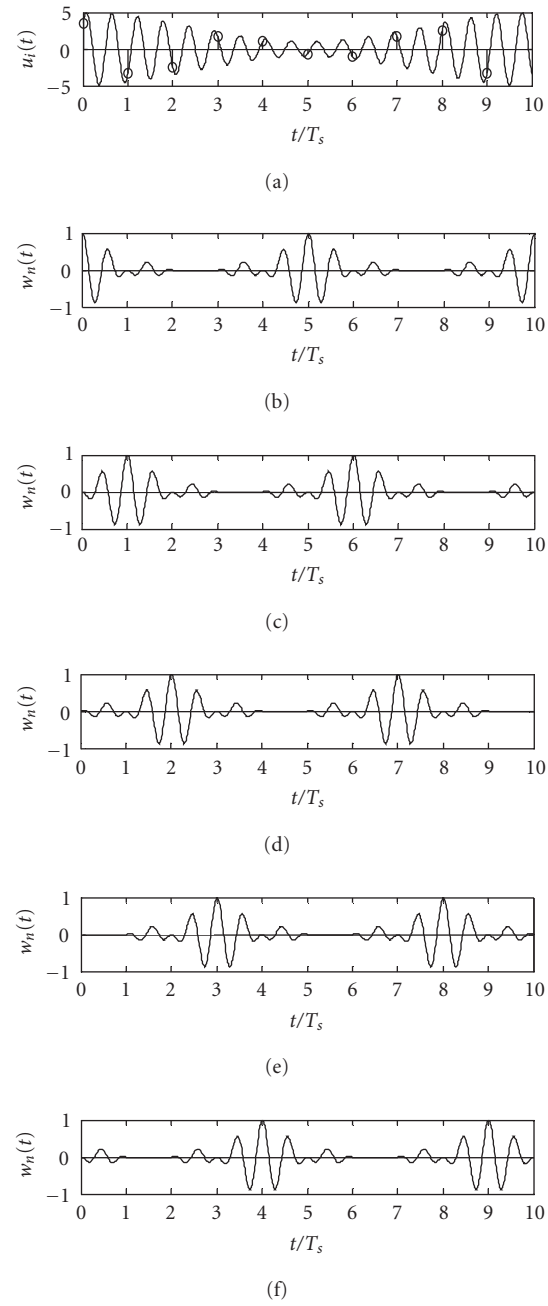

Figure 6: Positions of samples and corresponding $w_n(t)$.

by T_s. Positions of samples and corresponding $w_n(t)$ are illustrated by Figure 6 for $L = 5$. As follows from (7), $w_0(t)$ determines filtering properties of SCs. Examples of baseband and bandpass weight functions $w_0(t)$ and the AFRs $|G_a(f)|$ of the SCs with these $w_0(t)$ are shown in Figures 7 and 8, respectively. Since an SC performs finite impulse response (FIR) filtering with AFR $|G_a(f)|$, which is the amplitude spectrum of $w_0(t)$, it suppresses interference using zeros of its AFR. When baseband sampling takes place, the distances between the centers of adjacent intervals (2) and (3) are equal to f_s (see Figure 3). To suppress all intervals (3), $|G_a(f)|$ should

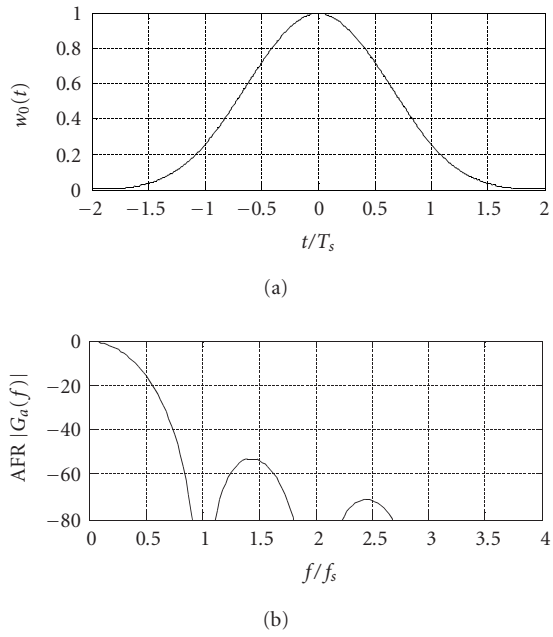

Figure 7: Baseband SC (a) $w_0(t)$ and (b) AFR $|G_a(f)|$, in dB.

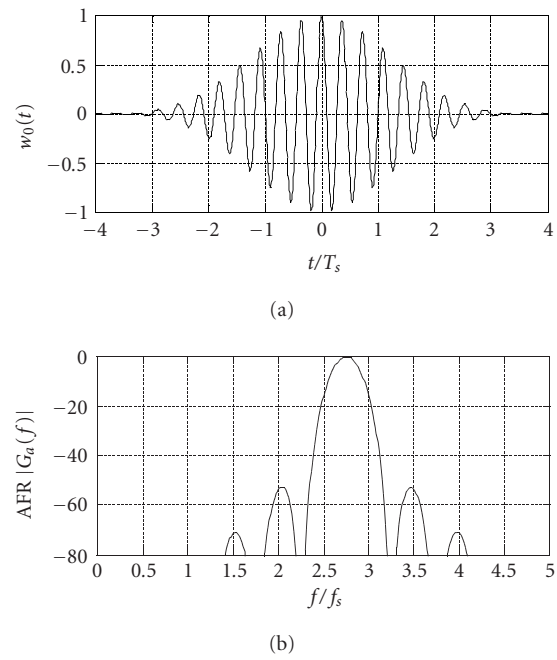

Figure 8: Bandpass SC (a) $w_0(t)$ and (b) AFR $|G_a(f)|$, in dB.

have at least one zero within each of them. To achieve this, condition $T_w \geq 1/f_s = T_s$ is necessary. For bandpass sampling, the distances between the centers of adjacent intervals (4) and (6) are equal to $0.5f_s$ (see Figure 4). Consequently, $T_w \geq 1/(0.5f_s) = 2T_s$ is required. When $T_h + T_c = T_s$, the length of the channel operational cycle is

$$\begin{aligned} LT_s &= T_w + T_h + T_c \geq 3T_s \quad \text{for bandpass } u(t), \\ LT_s &= T_w + T_h + T_c \geq 2T_s \quad \text{for baseband } u(t). \end{aligned} \tag{8}$$

It follows from (8) that $L \geq 3$ is required for bandpass sampling and $L \geq 2$ is necessary for baseband sampling. Only bandpass sampling is considered in the rest of the paper.

In the SC shown in Figure 5b, the required speed of A/Ds is lower and an analog Mx is replaced with a digital one. This version is preferable when the maximum speed of the A/Ds is lower than f_s, or when L slower A/Ds cost less and/or consume less power than faster one.

3.4. Canonical reconstruction circuits

The block diagrams of canonical RCs with internal filtering are shown in Figure 9. In Figure 9a, a demultiplexer (DMx) periodically (with period LT_s) connects the output of a D/A to each of L channels. The lth channel ($l \in [1, L]$) processes samples with numbers $l + kL$, where k is any integer. Operational cycle duration of each channel is equal to LT_s and delayed by T_s relative to that of the previous channel. The cycle consists of three modes: clear, sample, and multiply. In the clear mode, the SHA capacitor is discharged. Then, during the sample mode, this capacitor is connected to the D/A by the DMx and charged. Throughout these modes, there is no signal at the channel output because zero level enters the second input of a multiplier from a WFG. The reasonable total length of the sample and clear modes is equal to T_s. In the subsequent multiply mode with duration T_w, the signal from the SHA is multiplied by the appropriate copy of $w_0(t)$ generated by the WFG, and the product enters an adder that sums the output signals of all the channels. Since at any instant, $L - 1$ channels are in the multiply mode and one channel is in the sample or clear mode, the WFG simultaneously generates $L - 1$ copies of $w_0(t)$, each delayed by T_s relative to the previous one. The RC reconstructs an analog signal $u(t)$ according to the equation

$$u(t) \approx \sum_{n=-\infty}^{\infty} u(nT_s) \cdot w_n(t) = \sum_{n=-\infty}^{\infty} u(nT_s) \cdot w_0(t - nT_s). \tag{9}$$

It follows from (9) that the RC performs reconstruction filtering with transfer function determined by $w_0(t)$.

In the version of a canonical RC shown in Figure 9b, digital words are distributed by a digital DMx among L channels. Presence of a D/A in each channel allows removal of SHAs. Here, the channel operational cycle consists of two modes: convert and multiply. In the first mode, the D/A converts digital words into samples $u(nT_s)$, which are multiplied by $w_n(t)$ during the multiply mode. This version has the following advantages: lower requirements for the speed of D/As, replacement of an analog DMx by a digital one, and removal of SHAs.

3.5. Advantages of the SCs and RCs and challenges of their realization

Both SCs and RCs with internal filtering make AMPs highly adaptive and easily reconfigurable because $w_0(t)$, which determines their filtering properties, can be dynamically

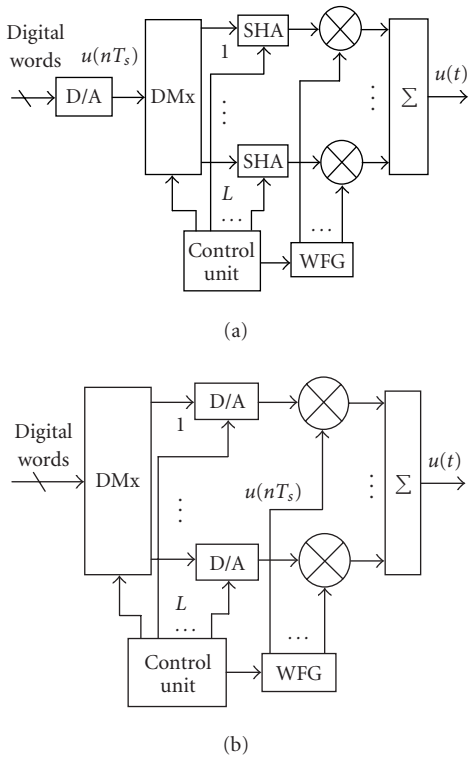

Figure 9: Canonical RCs with internal reconstruction filtering: (a) single-D/A version and (b) multiple-D/A version.

changed. Internal filtering performed by these structures allows removal of conventional antialiasing and reconstruction filters or their replacement by wideband low-selectivity filters realizable on a chip. This makes the AMP technology uniform and compatible with the IC technology. The RCs with internal filtering utilize the D/A output current more efficiently than conventional devices, then bandpass reconstruction takes place. The SCs with internal antialiasing filtering accumulate signal energy in their storage capacitors during the sample mode. This accumulation filters out jitter and reduces the charging current of the storage capacitors by 20–40 dB in most cases. Reduced jitter enables the development of faster A/Ds. The decrease in the charging current lowers both the required gain of an AMP and its nonlinear distortions. The reduced AMP gain allows sampling close to the antenna. Smaller charging current also lowers input voltage of the SCs. Indeed, although the same output voltage has to be provided by an SC with internal antialiasing filtering and a conventional SHA, the SC input voltage can be significantly lower when the integrator operational amplifier has an adequate gain. As mentioned in Section 2.1, a conventional SHA does not suppress out-of-band noise and IMPs of all the stages between the antialiasing filter and its capacitor. As a result of sampling, these noise and IMPs fall within the signal spectrum. The SCs with internal antialiasing filtering operate directly at the A/D input and reject out-of-band noise and IMPs of all preceding stages. Thus, they perform more effective antialiasing filtering than conventional structures.

At the same time, practical realization of the SCs and RCs with internal filtering and their implementation in SDRs present many technical challenges. Canonical structures of the SCs and RCs (see Figures 5 and 9) are rather complex. Therefore, their simplification is highly desirable. This simplification is intended, first of all, to reduce complexity and number of multiplications.

4. SIMPLIFICATION OF THE SCs AND RCs

4.1. Approaches to the problem

Approaches to simplification of the SCs and RCs depend on the ways of $w_n(t)$ generation and multiplications. Analog generation of $w_n(t)$ implies that multiplications of $u_i(t)$ in the SCs and $u(nT_s)$ in the RCs by $w_n(t)$ are performed by analog multipliers. Since only simple $w_n(t)$ can be generated by analog circuits, and this generation is not flexible enough, digital generation is preferable. When $w_n(t)$ are generated digitally, they can be converted to the analog domain in the WFG (see Figures 5 and 9) or sent to the multipliers in digital form. In the first case, multiplications in the SCs and RCs are analog. In the second case, these multiplications can be carried out by multiplying D/As.

Since digital $w_n(t)$ have unwanted spectral images, spectral components of an input signal $u_i(t)$ in the SCs and a reconstructed signal $u(t)$ in the RCs corresponding to the unwanted images should be suppressed. The suppression can be performed by a wideband filter with fairly low selectivity that allows IC implementation. Such a filter is sufficient because a required sampling rate of $w_0(t)$ representation is much higher than that of the A/D used in a receiver and the D/A used in a transmitter when bandpass sampling and reconstruction take place. In practice, some kind of prefiltering is performed in all types of receivers, and some kind of postfiltering is performed in transmitters. Usually, these prefiltering and postfiltering can provide the required suppression. Since prefiltering and postfiltering automatically suppress stopbands (6) remote from passband (4), internal filtering performed by SCs and RCs should first of all suppress stopbands (6) closest to the passband. Complexity of the SCs and RCs, caused by high sampling rate of $w_0(t)$ representation, can be compensated by its low resolution. The goal is to lower the required resolution of $w_0(t)$ representation or to find other means that can reduce multiplying D/As (or analog multipliers) to a relatively small number of switches.

Simplification of the SCs and RCs can be achieved by proper selection of $w_0(t)$ and optimization of their architectures for a given $w_0(t)$. Below, attention is mostly focused on the SCs because their practical realization is more difficult than that of RCs due to higher requirements for their dynamic range. Achieving a high dynamic range of multiplications in the SCs is still a challenging task, although low input current (compared to conventional SHAs) makes it easier.

Brief information on $w_0(t)$ selection is provided in Section 4.2, and two examples of the SC simplification are described and analyzed in Sections 4.3, 4.4, and 4.5. It is

important to emphasize that possible simplifications of the SCs are not limited to these examples.

4.2. Selection of weight functions

Selection of $w_0(t)$ is application specific and requires multiple tradeoffs. For example, $w_0(t)$ that maximizes the dynamic range of an AMP and $w_0(t)$ that provides the best internal filtering are different. Indeed, $w_0(t)$ with rectangular envelope maximizes the dynamic range due to its minimum peak factor and the most efficient accumulation of the signal energy, but it provides relatively poor internal filtering. At the same time, $w_0(t)$ that provides the best internal filtering for given L and f_s/B has high peak factor and relatively poor accumulation of signal energy. When both features are desirable, $w_0(t)$ has to be selected as a result of a certain tradeoff, and this result can be different depending on specific requirements for the radio. To provide the best antialiasing filtering for given L and f_s/B, $w_0(t)$ should be optimized using the least mean square (LMS) or Chebyshev criterion [23]. Any $w_0(t)$, optimal according to one of these criteria, requires high accuracy of its representation and multiplications. This complicates realization of the SCs. Suboptimal $w_0(t)$ that provide effective antialiasing filtering with low accuracy of representation and multiplications are longer than optimal $w_0(t)$ and, consequently, require larger L. An increase of f_s/B simplifies antialiasing filtering and allows reduction of L or accuracy of multiplications for a given quality of filtering [20]. Technology of the SCs and technical decisions regarding these and other units of the SDRs also influence selection of $w_0(t)$. Due to the complexity of these multiple tradeoffs, there is no mathematical algorithm for $w_0(t)$ selection, and heuristic procedures combined with analysis and simulation are used for this purpose.

In general, a bandpass $w_0(t)$ can be represented as

$$\begin{aligned} w_0(t) &= W_0(t)c(t) \quad \text{for } t \in [-0.5T_w, 0.5T_w], \\ w_0(t) &= 0 \quad \text{for } t \notin [-0.5T_w, 0.5T_w], \end{aligned} \tag{10}$$

where $W_0(t)$ is a baseband envelope, and $c(t)$ is a periodic carrier (with period $T_0 = 1/f_0$) that can be sinusoidal or nonsinusoidal. To provide linear phase-frequency response, $W_0(t)$ should be an even function, and $c(t)$ should be an even or odd function. Assuming that $T_w = kT_s$ where k is a natural number, we can expand $c(t)$ into Fourier series over the time interval $[-0.5T_w, 0.5T_w]$:

$$c(t) = \sum_{m=-\infty}^{\infty} c_m e^{jm2\pi f_0 t}, \tag{11}$$

where m is any integer and c_m are coefficients of the Fourier series. Taking into account (10) and (11), we can write that within the interval $[-0.5T_w, 0.5T_w]$,

$$w_0(t) = W_0(t) \sum_{m=-\infty}^{\infty} c_m e^{jm2\pi f_0 t} = \sum_{m=-\infty}^{\infty} w_{m0}(t), \tag{12}$$

where $w_{m0}(t)$ are partial weight functions, whose envelopes are equal to $c_m W_0(t)$ and whose carriers are harmonics of f_0. The spectra of $w_{m0}(t)$ are partial transfer functions $G_m(f)$. It follows from (12) that when f_0/f_s is high enough ($f_0/f_s > 3$ is usually sufficient), the distances between adjacent harmonics of f_0 are relatively large, and overlapping of $G_m(f)$ does not notably affect the suppression within those stopbands (6) that are close to the passband. Since remote stopbands (6) are suppressed by prefiltering or postfiltering, the simplest $c(t)$, which is a squarewave, can be used when f_0/f_s is sufficient. Combining a squarewave $c(t)$ with an appropriately selected K-level $W_0(t)$ allows reducing the multiplying D/As to a small number of switches. Note that, besides $w_0(t)$ with K-level $W_0(t)$, there are other classes of $w_0(t)$ that allow us to do this. If discontinuities in $W_0(t)$ and $c(t)$ are properly aligned and $f_0/f_s > 3$, overlapping of $G_m(f)$ can be insignificant even if condition $T_w = kT_s$ is not met.

The lower f_0/f_s is, the more significantly $G_m(f)$ are overlapped. As a result, both $W_0(t)$ and $c(t)$ influence the filtering properties of the SCs and RCs. When $f_0/f_s = 0.25$, $c(t)$ has the greatest impact on their transfer functions. To reduce the multiplying D/As to a small number of switches in this case, $c(t)$ should also be a several-level function.

4.3. Separate multiplying by $W_0(t)$ and $c(t)$

The following method of the SC realization can be obtained using separate multiplication of $u_i(t)$ by the envelope $W_0(t)$ and carrier $c(t)$ of $w_0(t)$. The nth sample at the output of the SC is as follows:

$$u(nT_s) = \int_{-0.5T_w+nT_s}^{0.5T_w+nT_s} u_i(t) w_0(t - nT_s)\, dt. \tag{13}$$

Taking into account (10), we can write

$$w_0(t - nT_s) = W_0(t - nT_s) \cdot c(t - nT_s). \tag{14}$$

When condition (5) is met, (14) can be rewritten as

$$w_0(t - nT_s) = W_0(t - nT_s) \cdot c\left[t - (n \bmod 4)\frac{T_0}{4}\right]. \tag{15}$$

Since $c(t \pm T_0/2) = -c(t)$,

$$c(t - nT_s) = \begin{cases} c(t)(-1)^{n/2} & \text{if } n \text{ is even}, \\ c\left(t - \dfrac{T_0}{4}\right)(-1)^{(n\pm1)/2} & \text{if } n \text{ is odd}. \end{cases} \tag{16}$$

Substituting (16) into (14), and (14) into (13), we obtain

$$u(nT_s) = \int_{-0.5T_w+nT_s}^{0.5T_w+nT_s} u_i(t) W_0(t - nT_s) \times \begin{cases} c(t)(-1)^{n/2} & \text{if } n \text{ is even} \\ c\left(t - \dfrac{T_0}{4}\right)(-1)^{(n\pm1)/2} & \text{if } n \text{ is odd} \end{cases} dt. \tag{17}$$

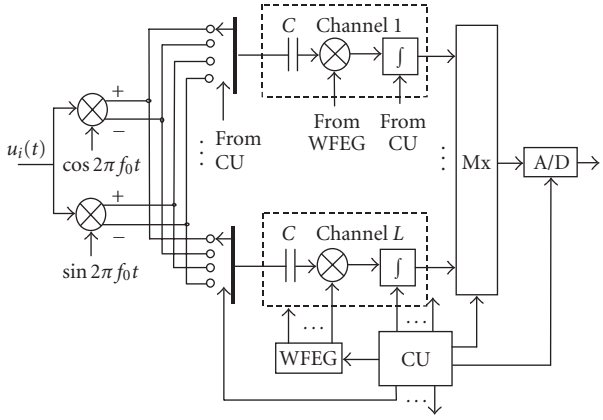

Figure 10: Modified SC.

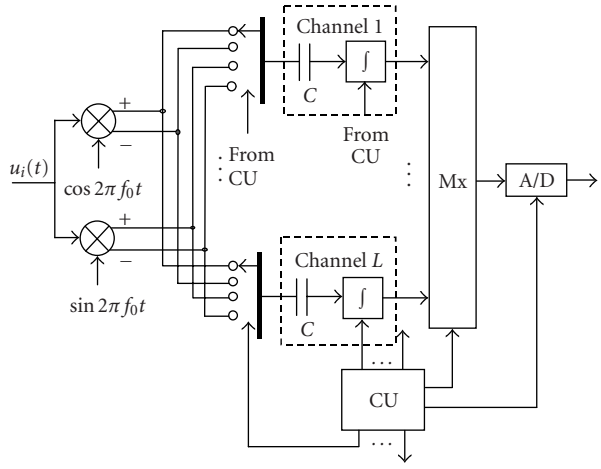

Figure 11: Modified SC with rectangular $W_0(t)$.

In (16) and (17), "±" corresponds to "±" in (5). In particular, when $c(t) = \cos 2\pi f_0 t$, (17) can be rewritten as follows:

$$u(nT_s) = \int_{-0.5T_w+nT_s}^{0.5T_w+nT_s} u_i(t) W_0(t - nT_s) \times \begin{Bmatrix} \cos(2\pi f_0 t)(-1)^{n/2} & \text{if } n \text{ is even} \\ \sin(2\pi f_0 t)(-1)^{(n\pm1)/2} & \text{if } n \text{ is odd} \end{Bmatrix} dt. \quad (18)$$

The algorithm described by (18) can be carried out by the modified SC shown in Figure 10. Here, $u_i(t)$ enters two multipliers where it is multiplied by $\cos 2\pi f_0 t$ and $\sin 2\pi f_0 t$. These multiplications are similar to the beginning of the procedure used for baseband sampling of bandpass signals (see Figures 1a and 1b). However, further processing is different. Instead of baseband filtering of the lowest spectral image after each multiplier, the differential outputs of both multipliers enter L channels through 4-contact switches. The switches are necessary because each sample in any channel is shifted by $\pm\pi L/2$ relative to the previous one in this channel when (5) is true. A control unit (CU) provides proper operation of the switches. This switching shifts the multiplier output spectral image from zero frequency to $f_s/4$. After passing decoupling capacitor C, it is processed in the channel. Similar to the canonical structure in Figure 5a, the operational cycle of each channel is equal to LT_s, consists of three modes (sample, hold, and clear), and is shifted by T_s relative to the operational cycle of the previous channel. The difference is that the channel input signal is multiplied by the appropriate copy $W_n(t)$ of $W_0(t)$ instead of $w_n(t)$ during the sample mode. A weight function envelope generator (WFEG) forms $W_n(t)$. Each $W_n(t)$ is shifted relative to the previous one by T_s to be in phase with the operational cycle of the corresponding channel.

At first glance, the structure in Figure 10 looks even more complex than the canonical one shown in Figure 5a. However, appropriate selection of $W_0(t)$ can significantly simplify it. For example, when $W_0(t)$ is a rectangular function, the WFEG and the multipliers in the channels are unnecessary. As shown in Figure 11, the modified SC contains only 2 multipliers for any L in this case. Complexity of the SC can also be lowered compared to the canonical structures when some other $W_0(t)$ are used. Note that single-ended circuits are used in Figures 10 and 11 only for simplicity of illustration. In practical applications, differential circuits are preferable.

4.4. Analysis of the modified SC

Many features of the canonical and modified SCs are the same. Indeed, when the same $w_0(t)$ are used, their filtering properties are identical and they accumulate equal amounts of signal energy. Consequently, they provide the same reduction of the input current compared to conventional sampling structures. They are equally adaptive and equally suitable for IC implementation. However, there is still substantial difference between them. A canonical SC is not sensitive to DC offset, while the outputs of the modified SCs are influenced by DC offsets in the first two multipliers. Besides, the number and values of IMPs that fall within the signal spectrum are higher in the modified SCs than in the canonical ones. Indeed, multiplication of $u_i(t)$ by $w_n(t)$ in each channel of the canonical SC creates a spectral image at the frequency $f_s/4$ because $w_n(t)$ are centered around corresponding sampling instants and f_s meets (5), whereas the first two multiplications in the modified SCs create baseband spectral images. Below, this is proven analytically.

Assuming that the DC offset in the multiplier of the lth channel in a canonical SC is U_l, where $l = [(n-1) \bmod L] + 1$, we can rewrite (13) as

$$u(nT_s) = \int_{-0.5T_w+nT_s}^{0.5T_w+nT_s} \left[u_i(t) w_0(t - nT_s) + U_l \right] dt. \quad (19)$$

It follows from (16) and (19) that

$$u(nT_s) = \int_{-0.5T_w+nT_s}^{0.5T_w+nT_s} u_i(t) W_0(t - nT_s) \times \begin{Bmatrix} c(t)(-1)^{n/2} & \text{if } n \text{ is even} \\ c\left(t - \dfrac{T_0}{4}\right)(-1)^{(n\pm1)/2} & \text{if } n \text{ is odd} \end{Bmatrix} dt + U_l T_w. \quad (20)$$

Equation (20) can be rewritten as

$$u(nT_s) = (-1)^{\text{floor}\,[(n+0.5\mp0.5)/2]} \int_{-0.5T_w+nT_s}^{0.5T_w+nT_s} u_i(t)W_0(t-nT_s) \times \begin{Bmatrix} c(t) & \text{if } n \text{ is even} \\ c\left(t+\dfrac{T_0}{4}\right) & \text{if } n \text{ is odd} \end{Bmatrix} dt + U_l T_w, \tag{21}$$

where sign "$\mp$" corresponds to "$\pm$" in (5). It follows from (21) that, at the output of a canonical SC, the component of the discrete-time signal, caused by the DC offset, is located at zero frequency, while its desired component is located at the frequency $f_s/4$, as indicated by coefficient $(-1)^{\text{floor}\,[(n+0.5\mp0.5)/2]}$. Thus, the DC offset can be easily filtered out in the receiver DP.

For the modified SC, we can write

$$u(nT_s) = \int_{-0.5T_w+nT_s}^{0.5T_w+nT_s} W_0(t-nT_s) \times \begin{Bmatrix} [u_i(t)c(t)+U_1](-1)^{n/2} & \text{if } n \text{ is even} \\ \left[u_i(t)c\left(t-\dfrac{T_0}{4}\right)+U_2\right](-1)^{(n\pm1)/2} & \text{if } n \text{ is odd} \end{Bmatrix} dt, \tag{22}$$

where U_1 and U_2 are DC offsets in the first two multipliers. Similar to (20), this equation can be rewritten as

$$u(nT_s) = (-1)^{\text{floor}\,[(n+0.5\mp0.5)/2]} \int_{-0.5T_w+nT_s}^{0.5T_w+nT_s} W_0(t-nT_s) \times \begin{Bmatrix} u_i(t)c(t)+U_1 & \text{if } n \text{ is even} \\ u_i(t)c\left(t+\dfrac{T_0}{4}\right)+U_2 & \text{if } n \text{ is odd} \end{Bmatrix} dt. \tag{23}$$

It follows from (23) that both signal and DC offset components after sampling are located at the frequency $f_s/4$, as indicated by coefficient $(-1)^{\text{floor}\,[(n+0.5\mp0.5)/2]}$. Therefore, the DC component cannot be filtered out.

Thus, DC offset and increased number and values of IMPs lower the performance of the modified SC compared to the canonical one. However, their performance is still significantly better than that of the conventional baseband sampling. Indeed, the entire signal processing is performed at zero frequency in the conventional procedure. Consequently, besides multipliers, all subsequent analog stages contribute to the increase in the DC offset and nonlinear distortion. In addition, baseband antialiasing filters create significant phase imbalance between I and Q channels. In the modified SCs, signal processing after 4-contact switches is performed at $f_s/4$, and subsequent analog stages do not increase nonlinear distortions and DC offset. The phase mismatch among channels of the modified SC is negligible because all clock impulses are generated in the control unit using the same reference oscillator, and proper design allows us to minimize time skew. As follows from Section 4.2, $\cos 2\pi f_0 t$ and $\sin 2\pi f_0 t$ in the first two multipliers of the modified SC can be replaced by squarewaves with frequency f_0 and time shift of $0.25T_0 = 0.25/f_0$ relative to each other when $f_0/f_s > 3$, and sufficient prefiltering is provided. This replacement further simplifies the modified SCs. Thus, the described modification of the SCs substantially simplifies their realization at the expense of slightly lower performance.

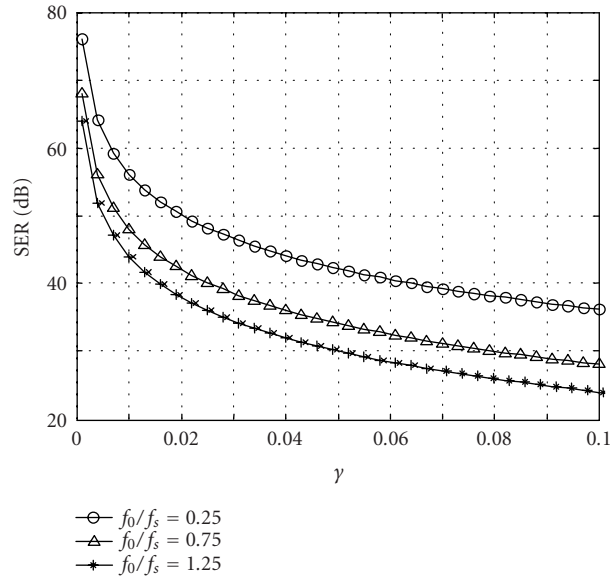

Figure 12: SER(γ) for various f_0/f_s.

4.5. Use of orthogonality of WFG outputs

As mentioned in Section 4.2, increase of f_s/B makes internal filtering easier and may allow reduction of L. In addition to reducing L, high-ratio f_s/B makes possible reducing the number of multipliers N for given L if f_0/B is also high. This possibility is discussed below.

When (5) is true, the carrier of $w_n(t)$ generated for nth sample is rotated by $\pm\pi/2$ relative to the carrier of $w_{n+2m+1}(t)$ generated for $(n+2m+1)$th sample, where m is any integer. Thus, if the envelope of $w_0(t)$ is rectangular, in some cases, $w_n(t)$ and $w_{n+2m+1}(t)$ can be sent to the same multiplier of the SC or RC with internal filtering even when these weight functions overlap. This property can be used to reduce N for a given L. For example, if $T_w/T_s = 2$ ($L = 3$) and $u(t) = U_0\cos(2\pi f_0 t + \varphi_0)$, one multiplier can be used for all 3 channels and perform, ideally accurate sampling. However, a pure sinewave cannot carry information. In the case of a bandpass signal $u(t) = U(t)\cos[2\pi f_0 t + \varphi(t)]$, sampling error is unavoidable, and signal-to-error power ratio (SER) for this error is

$$\text{SER} = \frac{16\pi^2}{\gamma^2}\left[\frac{(\pi f_0 T_w)^2 - 1}{(\pi f_0 T_w)^3 \mp 1}\right]^2 \tag{24}$$

when $B \ll 1/T_w$. Here, "$\mp$" corresponds to "$\pm$" in (5), $\gamma = B_{\text{RMS}}/f_0$, and B_{RMS} is root mean square bandwidth of $u(t)$. Figure 12 illustrates the dependence SER(γ) for several values

of f_0/f_s. Since the spectrum of the error determined above is generally wider than $S_u(f)$, a part of this error can be filtered out in the receiver DP. Therefore, (24) is a lower bound of the actual SER.

This method of reducing the number of multipliers N can also be used for $L > 3$ if the corresponding SER is sufficiently small. In this case, the minimally required N is

$$N = \begin{cases} \dfrac{0.5T_w}{T_s} + 1 & \text{if } \dfrac{0.5T_w}{T_s} \text{ is even,} \\ \dfrac{0.5T_w}{T_s} & \text{if } \dfrac{0.5T_w}{T_s} \text{ is odd.} \end{cases} \tag{25}$$

For $N > 1$, this method can complicate the channel mismatch compensation in the receiver DP described in the next section. It is important to mention that (24) can be used for any N.

It follows from (24) and Figure 12 that the described method can be used only with very high-ratios f_s/B that correspond exclusively to sigma-delta A/Ds.

5. CHANNEL MISMATCH MITIGATION

5.1. Approaches to the problem

The SCs and RCs with internal filtering are inherently multichannel. Therefore, the influence of channel mismatch on the performance of SDRs must be minimized. This is especially important for the SUs because in the receivers, $u(t)$ is a sum of a desired signal $s(t)$ and a mixture of the noise and interference $n(t)$. Thus, $u(t) = s(t) + n(t)$. When the average power of $n(t)$ is larger than that of $s(t)$, the average power of the error $e(t)$ caused by the channel mismatch can be comparable with or even exceed the power of $s(t)$.

There are three approaches to this problem. The first of them includes technical and technological measures that reduce this mismatch: placing all the channels on the same die, simplifying $w_0(t)$, and correcting circuit design. The second approach is based on preventing an overlap of the signal and mismatch error spectra. In this case, the error spectrum can be filtered out in the DP. The third approach is adaptive compensation of the channel mismatch in the DP. The first approach alone is sufficient for many types of transmitters and for receivers with limited dynamic range. In high-quality receivers, the measures related to this approach are necessary but usually not sufficient. Therefore, the second and third approaches are considered below.

5.2. Separation of signal and error spectra

To determine the conditions that exclude any overlap between spectra $S_{u1}(f)$ of $u(nT_s)$ and $S_e(f)$ of $e(t)$, we first find $S_e(f)$. The phase mismatch among channels can be made negligible because all clock impulses are generated in the control unit using the same reference oscillator, and proper design minimizes time skew. Therefore, it is sufficient to take into account only the amplitude mismatch caused by the differences among the channel gains $g_1, g_2, \ldots, g_L$. The average gain is $g_0 = (g_1 + g_2 + \cdots + g_L)/L$, and the deflection from g_0 is

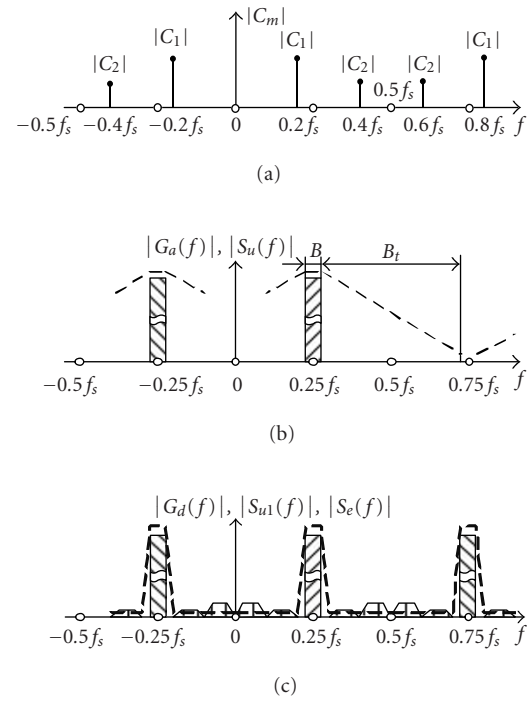

Figure 13: Amplitude spectra and AFRs: (a) spectral components of $d(t)$; (b) $|S_u(f)|$—solid line, $|G_a(f)|$—dashed line; (c) $|S_{u1}(f)|$ and $|S_e(f)|$—solid line, $|G_d(f)|$—dashed line.

$d_l = g_l - g_0$ in the lth channel. Since samples of $u(t)$ are generated in turn by all channels, the deflections $d_1, d_2, \ldots, d_L, d_1, d_2, \ldots, d_L, d_1, d_2, \ldots$ appear at sampling instants $t = nT_s$ as a periodic function $d(t)$ with period LT_s:

$$d(t) = \sum_{k=-\infty}^{\infty} \sum_{l=1}^{L} \{d_l \delta[t - (kL + l)T_s]\}, \tag{26}$$

where $\delta(t)$ is the delta function. The spectrum of $d(t)$ is

$$S_d(f) = \sum_{m=-\infty}^{\infty} \left[C_m \delta\left(f - \frac{m}{L} f_s \right) \right], \tag{27}$$

where coefficients

$$C_m = \frac{1}{LT_s} \sum_{l=1}^{L} \left[d_l \exp\left(\frac{-j2\pi ml}{L} \right) \right]. \tag{28}$$

As reflected by (27) and (28), $S_d(f)$ is a periodic function with the period f_s because $d(t)$ is discrete with sampling period T_s. Therefore, it is sufficient to consider $S_d(f)$ only within the interval $[-0.5f_s, 0.5f_s[$. Since $d(t)$ is real-valued, $S_d(f)$ is even. Since $d(t)$ is periodic with period LT_s, $S_d(f)$ is discrete with the harmonics located at frequencies $\pm mf_s/L$, $m = 1, 2, \ldots,$ floor $(L/2)$ within the interval $[-0.5f_s, 0.5f_s[$. The spectral components of $d(t)$ are shown in Figure 13a for $L = 5$. When (5) is true, the images of the spectrum $S_{u1}(f)$

of $u(nT_s)$ occupy the following bands within the interval $[-0.5f_s, 0.5f_s[$:

$$\begin{aligned}&[-0.25f_s - 0.5B, -0.25f_s + 0.5B]\\ &\quad\cup [0.25f_s - 0.5B, 0.25f_s + 0.5B],\end{aligned} \tag{29}$$

where B is a bandwidth of $u(t)$. Figure 13b shows $|S_u(f)|$ and the AFR $|G_a(f)|$ of antialiasing filtering performed by the SC for $f_0 = 0.25f_s$. Spectrum $S_e(f)$ is a convolution of $S_u(f)$ and $S_d(f)$. Taking (5) into account, we get

$$\begin{aligned}S_e(f) = \sum_{m=-\infty}^{\infty} \Bigg\{ C_m \Bigg\{ S_u\left[f - f_s\left(\frac{m}{L} - 0.25\right)\right]\\ + S_u\left[f - f_s\left(\frac{m}{L} + 0.25\right)\right]\Bigg\}\Bigg\}.\end{aligned} \tag{30}$$

Since $e(t)$ is a real-valued discrete function with sampling period T_s, $|S_e(f)|$ is an even periodic function with the period f_s that is unique within the interval $[-0.5f_s, 0.5f_s[$.

It follows from (30) that if L is even, the error image corresponding to $m = \pm L/2$ falls to the frequencies $\pm 0.25f_s$, that is, within the signal spectrum. Therefore, $S_e(f)$ and $S_u(f)$ cannot be separated. When L is odd, the situation is different. The centers of the images caused by the channel mismatch are located at frequencies $\pm(r + 0.5)f_s/(2L)$, where $r = 0, 1, \ldots, 0.5(L-1) - 1, 0.5(L-1) + 1, \ldots, L - 1$ within the interval $[-0.5f_s, 0.5f_s[$. The bandwidth of each image is $B_1 = B + 2B_{t1}$, where B_{t1} is the image one-sided transition band. The images of $S_e(f)$ are created by coefficients C_m. Since these coefficients are different, the images have different transition bands. However, we assume for simplicity that transition bands of all images are equal to those of the most powerful image. Mean values of $u(t)$ and $e(t)$ are equal to zero. Denoting the standard deviation of $u(t)$ and $e(t)$ as σ_u and σ_e, respectively, we can state that $\sigma_u \gg \sigma_e$. The standard deviation σ_{e1} of the most powerful spectral image of $e(t)$ always meets condition $\sigma_{e1} \le \sigma_e$. It is reasonable to assume $B_t/B_{t1} = \sigma_u/\sigma_{e1} = M$ where B_t is the antialiasing-filter one-sided transition band. Thus, $B_{t1} = B_t/M$ and $M > 1$. Taking into account that $B_t \le 0.5f_s - B$, we obtain

$$B_1 \le B + 2\left[\frac{(0.5f_s - B)}{M}\right]. \tag{31}$$

Since channel filtering in the receiver DP removes all the spectral components of $e(t)$ outside bands (29), only the part of $S_e(f)$ which falls within these bands degrades the receiver performance. It follows from (29) and (30) that $S_e(f)$ and $S_u(f)$ do not overlap if $(B + B_1) \le f_s/L$. Inequality (31) allows us to rewrite this condition as follows:

$$\frac{f_s}{B} \ge 2L\frac{(M-1)}{(M-L)} \quad \text{and} \quad M \ge L. \tag{32}$$

According to (32), $f_s/B \to 2L$ when $M \to \infty$. In practice, $M \ge 100$. Table 3 shows the minimum values of f_s/B required to filter out $e(t)$ when L is odd. It follows from Table 3 that it is relatively easy to avoid an overlap of $S_e(f)$ and $S_u(f)$ and exclude an impact of the SC channel mismatch on the receiver performance when $L = 3$. For odd $L > 3$, significant increase of f_s is required. Consequently, combining the SCs and sigma-delta A/Ds almost automatically excludes this impact if L is odd.

Table 3: Minimum values of f_s/B.

$M \downarrow$	$L \rightarrow$	3	5	7	9	11
100	f_s/B	6.1	10.4	14.9	19.6	24.5
1000	f_s/B	6.01	10.04	14.08	18.15	22.22

When L is odd, but (32) is not met, $S_e(f)$ and $S_u(f)$ overlap. However, the overlap can be lowered by increasing f_s/B and, when $L \ge 5$, by reducing the $S_d(f)$ harmonics adjacent to $\pm 0.5f_s$ since they create the closest-to-the-signal images of $S_e(f)$. Changing the succession of channel switching can reduce the harmonics. The succession that makes $d(t)$ close to a sampled sinewave minimizes the overlap.

Figure 13c shows $|S_{u1}(f)|$ and $|S_e(f)|$ for the situation when L is odd and condition (32) is met. Here, the error images adjacent to the signal are created by C_2, and the more distant images by C_1. The AFR $|G_d(f)|$ of the DP channel filter is shown by the dashed line.

5.3. Compensation of channel mismatch in DP

If, despite all the measures, the residual error caused by the mismatch still degrades the receiver performance, it can be adaptively compensated in the DP. This compensation can be performed either during the operation mode simultaneously with signal processing or during a separate calibration mode. In all cases, channel gains g_l are estimated first, and then deflections d_l are compensated.

There are many methods of fast channel gain estimation in calibration mode. For example, when all the copies $w_n(t)$ of $w_0(t)$ are simultaneously applied to the SC multipliers and a test signal is sent to the SC input, estimation time is $T_e = T_w + LT_s = (2L-1)T_s$, assuming that T_s is required for the hold and clear modes in each channel. A sinewave with frequency f_0 is the simplest test signal. The estimation can also be done when $w_n(t)$ are delayed relative to each other by T_s, like in the operational mode. If (5) is true and the test signal is a sinewave with frequency f_0 and arbitrary initial phase, $T_e = 2T_w + (L+1)T_s = (3L-1)T_s$ because two consecutive samples are required for each channel to estimate its gain. When the phase shift between the sinewave and the carrier of $w_0(t)$ is equal to $\pm 45°$, the estimation time can be reduced to $T_e = T_w + LT_s = (2L-1)T_s$.

Channel mismatch compensation performed during the operation mode requires much longer estimation because $u(t)$ is a stochastic process. The block diagram of a simplified version of such a compensator is shown in Figure 14. Here, a demultiplexer (DMx) distributes digital words resulting from the SC samples among L digital channels. Each digital channel corresponds to the SC channel with the same number. Averaging units (AU) calculate the mean magnitudes of samples in each channel. The mean magnitudes are processed

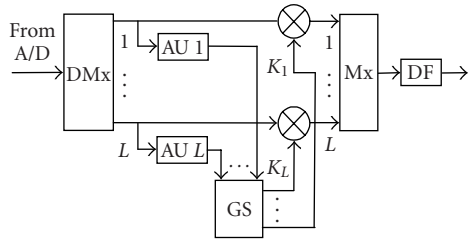

Figure 14: Digital channel mismatch compensator.

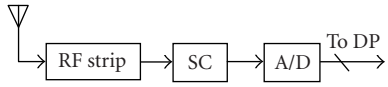

Figure 15: Modified receiver AMP architecture with digitization at the RF.

in a gain scaler (GS), which generates coefficients K_l that compensate the channel mismatch. A multiplexer (Mx) combines the outputs of all the channels. A subsequent digital filter (DF) provides the main frequency selection. In practice, channel mismatch compensation during the operation mode requires the most statistically efficient methods of g_l estimation, and the compensator should be designed together with automatic gain control (AGC) of the receiver.

6. AMPS' ARCHITECTURES BASED ON SAMPLING AND RECONSTRUCTION WITH INTERNAL FILTERING

6.1. General

It is shown in Section 2 that the SDR front ends with bandpass sampling, reconstruction, and antialiasing filtering potentially provide the best performance. At the same time, conventional methods of sampling, reconstruction, and filtering limit flexibility of the front ends, complicate their IC implementation, and do not allow achieving their potential parameters. It follows from Section 3 that implementation of the novel sampling and reconstruction techniques with internal filtering can eliminate these drawbacks and provide some additional benefits. Sections 4 and 5 demonstrate that challenges of the proposed techniques realization can be overcome. The impact of these techniques on the architectures of the radios' AMPs is discussed below.

6.2. Modified receiver AMPs

Implementation of sampling with internal antialiasing filtering in digital receivers requires modification of their front ends. Since accumulation of the signal energy in the storage capacitors of the SCs significantly reduces the required gain of AMPs, and antialiasing filtering performed by the SCs is flexible, it is reasonable to consider the possibility of signal digitization at the receiver RF. This leads to the simplest AMP architecture shown in Figure 15. Here, an RF strip performs prefiltering and all the required amplification, an SC carries out antialiasing filtering and sampling, and an A/D quantizes the output of the SC. All further processing is performed in a DP.

When multiplication of $u_i(t)$ by $w_0(t)$ is performed in the analog domain, the carrier $c(t)$ of $w_0(t)$ is a sinewave, the envelope $W_0(t)$ of $w_0(t)$ is a smooth function, and the AMP has sufficient dynamic range, prefiltering in the RF strip is used only to limit the receiver frequency range R. The same type of prefiltering can be used when $c(t)$ is nonsinusoidal and/or $W_0(t)$ is not a smooth function, but R is narrower than half an octave. Such prefilters do not require any adjustment during frequency tuning.

If the conditions above are not met, the prefilter bandwidth should be narrower than R. Nonsinusoidal $c(t)$ and nonsmooth $W_0(t)$ require the prefilter bandwidth that does not exceed half an octave. In practice, the prefilter bandwidth is determined as a result of a tradeoff. Indeed, on the one hand, reduction of the prefilter bandwidth allows increasing its transition band. This simplifies IC implementation of the prefilter. On the other hand, increase in the prefilter bandwidth simplifies its frequency tuning.

In any case, signal $u(t)$ intended for digitization is only a part of $u_i(t)$, and $u(t)$ usually has wider spectrum than a desired signal $s(t)$ since channel filtering is performed in the DP. Therefore, a reasonable algorithm of the automatic gain control (AGC) is as follows. The RF strip gain should be regulated by a control signal generated at the output of a digital channel filter and constraints generated at the input of the SC and at the output of the D/A. These constraints prevent clipping of $u(t)$ caused by powerful interference, which is filtered out by the digital channel filter, and clipping of $u_i(t)$ caused by powerful interference, which is filtered out by the SC. To compensate level variations due to the constraints, feed-forward automatic scaling is usually required in the DP with fixed-point calculations.

Reconfiguration or adaptation of the receiver at the same f_0 usually can be achieved by varying only $W_0(t)$. Frequency tuning requires shifting the AFR of the SC along the frequency axis and, sometimes, adjusting the prefilter AFR. The AMP has to carry out only coarse frequency tuning. Fine tuning with the required accuracy can be performed in the receiver DP. The reasonable increment Δf of coarse tuning is about $0.1B$, where B is the bandwidth of $u(t)$. Thus, the number of different center frequencies f_0 within the frequency range R is about $10\,R/B$. In most cases, coarse tuning requires changing both $c(t)$ and $W_0(t)$. Indeed, when f_0 is changed, usually f_s should also be changed to preserve condition (5). This in turn necessitates changing $W_0(t)$ because certain relations between f_s and T_w are necessary to suppress noise and interference within intervals (6). During coarse tuning, $W_0(t)$ can remain unchanged only when previous and subsequent frequencies f_0 have the same optimal f_s and keeping unchanged $W_0(t)$ does not cause additional discontinuities in $w_0(t)$. However, this happens rarely, and frequency tuning in the AMP shown in Figure 15 is relatively complex. The SCs described in Section 4.3 cannot be used in this architecture due to possible leakage of the $c(t)$ generator.

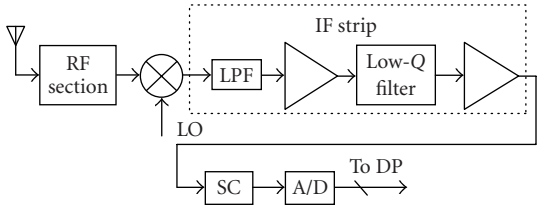

Figure 16: Modified superheterodyne receiver AMP architecture with sampling at the IF.

A superheterodyne architecture of the receiver AMP modified to accommodate sampling with internal antialiasing filtering at the IF is shown in Figure 16. Compared to the previous architecture, this one simplifies both frequency tuning and prefiltering. Here, an RF section performs image rejection and preliminary amplification of the sum of a desired signal, noise, and interference. Prefiltering and further signal amplification are carried out in an IF strip. This prefiltering is performed by a filter with low quality factor (Q) that can be implemented on a chip.

In principle, prefiltering is necessary only when $c(t)$ is nonsinusoidal and/or $W_0(t)$ is not a smooth function. Otherwise, it can be excluded. However, as shown in Section 4.2, use of a K-level $W_0(t)$ and a squarewave carrier $c(t)$ radically simplifies the SC due to reducing multiplying D/As to a relatively small number of switches. Besides, it allows increasing the receiver IF, which, in turn, simplifies image rejection in the RF section. When the receiver frequency range R is wide, a variable IF allows avoiding spurious responses. In practice, two or three different f_0's are sufficient, and they can be selected so that transitions from one f_0 to another require minimum adjustment. For example, these transitions may require changing only $c(t)$. If these frequencies are within the bandwidth of the low-Q filter, the latter does not require any adjustment when the IF is changed. In both AMP architectures shown in Figures 15 and 16, all measures that reduce the influence of the SC channel mismatch on the receiver performance (see Section 5) should be taken. Therefore, when condition (32) is not met, digital channel mismatch compensator has to be implemented in the receiver DP.

Despite the differences, the AMP architectures in Figures 15 and 16 utilize the advantages of sampling with internal antialiasing filtering (see Section 3.5). First of all, removal of high-quality conventional antialiasing filters (e.g., SAW, crystal, mechanical, ceramic) and implementation of the SCs with variable $w_0(t)$ make these architectures realizable on a chip, reconfigurable, and adaptive. Then, the proposed sampling significantly improves performance by adding to the benefits of bandpass sampling described in Section 2.1 the following advantages. A variable IF allows avoiding spurious responses in a superheterodyne AMP. Nonlinear distortions are radically reduced due to rejection of out-of-band IMPs of all preceding stages and lower input current of the SC caused by accumulation of the signal energy. This accumulation also filters out jitter, improving performance and speed of the A/D. Finally, the accumulation of signal energy lowers the required AMP gain and allows sampling close to the antenna.

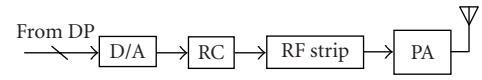

Figure 17: Modified transmitter AMP architecture with reconstruction at the RF.

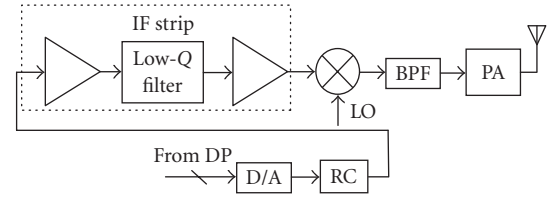

Figure 18: Modified offset up-conversion transmitter AMP architecture with reconstruction at the IF.

6.3. Modified transmitter AMPs

Similar to the case of receivers, implementation of reconstruction with internal filtering in transmitters requires modification of their AMPs. This modification affects only the transmitter drive (exciter) and does not influence the transmitter PA. Signal reconstruction at the transmitter RF leads to the simplest AMP architecture shown in Figure 17. Here, digital words corresponding to the samples of a bandpass signal are formed in a DP at the transmitter RF. Then, they are converted to the analog samples by a D/A. An RC reconstructs the bandpass analog signal and carries out main analog filtering. A subsequent RF strip amplifies the signal to the level required at the input of a PA and performs postfiltering. This postfiltering is absolutely necessary when $c(t)$ is nonsinusoidal and/or $W_0(t)$ is not a smooth function. Although the AMP in Figure 17 looks simple, its implementation causes problems related to frequency tuning of the transmitter and digital-to-analog conversion of bandpass signals at the varying RF.

These problems are solved in the offset up-conversion AMP architecture modified to accommodate bandpass reconstruction with internal filtering at the IF shown in Figure 18. The fact that reconstruction, preliminary amplification, and postfiltering of bandpass analog signals are carried out at the transmitter IF significantly simplifies realization of this procedures. An RC performs main reconstruction filtering, while postfiltering is carried out by a low-Q IF filter that can be placed on a chip.

Implementation of reconstruction with internal flexible filtering makes the transmitter AMPs easily reconfigurable and highly adaptive and increases their scale of integration. This reconstruction also reduces the required AMP gain due to more efficient utilization of the D/A output current. As a result, reconstruction can be performed closer to the antenna than in conventional architectures.

7. CONCLUSIONS

In modern SDRs, analog front end architectures with bandpass sampling, reconstruction, and antialiasing filtering can

potentially provide the best performance of both receivers and transmitters. However, conventional methods of performing these procedures limit flexibility, complicate IC implementation, and do not allow achieving the potential performance of the radios.

Novel sampling and reconstruction techniques with internal filtering derived from the sampling theorem eliminate these problems. The techniques provide high flexibility because their filtering and other properties are determined by weight functions $w_0(t)$ that can be dynamically changed. Since technology of the SCs and RCs with internal filtering is compatible with IC technology, they radically increase scale of integration in the AMPs. The RCs provide more efficient utilization of the D/A output current than conventional techniques. The SCs accumulate the input signal energy. This accumulation filters out jitter, improving performance and speed of A/Ds, and reduces the input current. The reduction of the input current lowers nonlinear distortions and required gain of AMPs.

Technical challenges of the SCs and RCs practical realization can be overcome by proper selection of $w_0(t)$ and optimization of their architectures for a given $w_0(t)$. Selection of $w_0(t)$ requires multiple tradeoffs. Simplification of the SCs and RCs is usually intended to reduce complexity and/or number of multiplications. Minimum complexity of multiplications is achieved when multiplying D/As or analog multipliers can be replaced by a relatively small number of switches. This can be accomplished, for instance, by using $w_0(t)$ with K-level envelope $W_0(t)$ and squarewave carrier $c(t)$ when $W_0(t)$ and $c(t)$ are properly synchronized and f_0/f_s is adequately high ($f_0/f_s > 3$ is usually sufficient). When f_0/f_s is low, $c(t)$ should also be a several-level function. There are other classes of $w_0(t)$ that allow replacing multipliers by a small number of switches.

Separate multiplications of the input signal $u_i(t)$ by $W_0(t)$ and $c(t)$ and use of only two multipliers for multiplying by $c(t)$ lead to a method that significantly simplifies the SCs. Although this is achieved at the expense of slightly reduced performance compared to the canonical SCs, the simplified SCs still provide significantly better performance of the radios than conventional sampling.

Increase of f_s/B simplifies antialiasing and reconstruction filtering and allows reduction of L in some cases. When both f_s/B and f_0/B are sufficiently high, use of WFG outputs' orthogonality allows reduction of N for a given L. However, this method is practical only for very high f_s/B.

Since SCs and RCs with internal filtering are inherently multichannel, the impact of channel mismatch on the performance of SDRs should be minimized. There are three approaches to the problem. The first of them includes all technical and technological measures that reduce the mismatch. The second one is based on preventing an overlap of signal and mismatch error spectra. This can be achieved only when L is odd, and condition (32) is met. In this case, the error spectrum can be filtered out in the DP. Combination of the SCs with odd L and sigma-delta A/Ds almost automatically excludes the overlap. When L is odd, but condition (32) is not met, the overlap cannot be avoided. However, it can be lowered by increasing f_s/B and, when $L \geq 5$, by reducing the $S_d(f)$ harmonics adjacent to $\pm 0.5 f_s$. The third approach is based on adaptive compensation of the channel mismatch in the DP.

In principle, sampling and reconstruction with internal filtering can be carried out at the radios' RFs. However, frequency conversion to an IF significantly simplifies practical realization of the modified SDRs.

Implementation of the SCs and RCs with internal filtering in SDRs radically increases reconfigurability, adaptivity and scale of integration of their front ends. Simultaneously, it improves performance of the radios due to significant reduction of nonlinear distortions, rejection of out-of-band noise and IMPs of all stages preceding sampling, avoiding spurious responses, and filtering out jitter. This implementation also substantially reduces front ends of SDRs, enabling sampling and reconstruction close to the antenna.

REFERENCES

[1] T. Anderson and J. W. Whikohart, "A digital signal processing HF receiver," in *Proc. 3rd International Conference on Communication Systems & Techniques*, pp. 89–93, London, UK, February 1985.

[2] C. M. Rader, "A simple method for sampling in-phase and quadrature components," *IEEE Trans. Aerosp. Electron. Syst.*, vol. 20, no. 6, pp. 821–824, 1984.

[3] M. V. Zarubinskiy and Y. S. Poberezhskiy, "Formation of readouts of quadrature components in digital receivers," *Telecommunications and Radio Engineering*, vol. 40/41, no. 2, pp. 115–118, 1986.

[4] Y. S. Poberezhskiy, *Digital Radio Receivers*, Radio & Communications, Moscow, Russia, 1987 (Russian).

[5] J. B.-Y. Tsui, *Digital Microwave Receivers: Theory and Concepts*, Artech House, Norwood, Mass, USA, 1989.

[6] M. E. Frerking, *Digital Signal Processing in Communication Systems*, Van Nostrand Reinhold, New York, NY, USA, 1994.

[7] W. E. Sabin and E. O. Schoenike, Eds., *Single-Sideband Systems and Circuits*, McGraw-Hill, New York, NY, USA, 2nd edition, 1995.

[8] J. Mitola III, "The software radio architecture," *IEEE Commun. Mag.*, vol. 33, no. 5, pp. 26–38, 1995.

[9] R. I. Lackey and D. W. Upmal, "Speakeasy: the military software radio," *IEEE Commun. Mag.*, vol. 33, no. 5, pp. 56–61, 1995.

[10] B. Razavi, "Recent advances in RF integrated circuits," *IEEE Commun. Mag.*, vol. 35, no. 12, pp. 36–43, 1997.

[11] H. Meyr, M. Moeneclaey, and S. A. Fechtel, *Digital Communications Receivers*, John Willey & Sons, New York, NY, USA, 1998.

[12] A. A. Abidi, "CMOS wireless transceivers: the new wave," *IEEE Commun. Mag.*, vol. 37, no. 8, pp. 119–124, 1999.

[13] J. Mitola III, *Software Radio Architecture*, John Willey & Sons, New York, NY, USA, 2000.

[14] C. Chien, *Digital Radio Systems on a Chip: a System Approach*, Kluwer Academic, Boston, Mass, USA, 2000.

[15] M. Helfenstein and G. S. Moschytz, Eds., *Circuits and Systems for Wireless Communications*, Kluwer Academic, Boston, Mass, USA, 2000.

[16] Y. Sun, Ed., *Wireless Communication Circuits and Systems*, IEE, London, UK, 2004.

[17] Y. S. Poberezhskiy and G. Y. Poberezhskiy, "Sampling with weighted integration for digital receivers," in *Proc. Digest of*

IEEE MTT-S Symposium on Technologies for Wireless Applications, pp. 163–168, Vancouver, British Columbia, Canada, February 1999.

[18] Y. S. Poberezhskiy and G. Y. Poberezhskiy, "Sampling technique allowing exclusion of antialiasing filter," *Electronics Letters*, vol. 36, no. 4, pp. 297–298, 2000.

[19] Y. S. Poberezhskiy and G. Y. Poberezhskiy, "Sample-and-hold amplifiers performing internal antialiasing filtering and their applications in digital receivers," in *Proc. IEEE Int. Symp. Circuits and Systems (ISCAS '00)*, vol. 3, pp. 439–442, Geneva, Switzerland, May 2000.

[20] Y. S. Poberezhskiy and G. Y. Poberezhskiy, "Sampling algorithm simplifying VLSI implementation of digital receivers," *IEEE Signal Processing Lett.*, vol. 8, no. 3, pp. 90–92, 2001.

[21] Y. S. Poberezhskiy and G. Y. Poberezhskiy, "Signal reconstruction technique allowing exclusion of antialiasing filter," *Electronics Letters*, vol. 37, no. 3, pp. 199–200, 2001.

[22] Y. S. Poberezhskiy and G. Y. Poberezhskiy, "Sampling and signal reconstruction structures performing internal antialiasing filtering," in *Proc. 9th International Conference on Electronics, Circuits and Systems (ICECS '02)*, vol. 1, pp. 21–24, Dubrovnik, Croatia, September 2002.

[23] Y. S. Poberezhskiy and G. Y. Poberezhskiy, "Sampling and signal reconstruction circuits performing internal antialiasing filtering and their influence on the design of digital receivers and transmitters," *IEEE Trans. Circuits Syst I: Regular Papers*, vol. 51, no. 1, pp. 118–129, 2004, erratum ibid. vol. 51, no. 6, p. 1234, 2004.

Yefim S. Poberezhskiy received the M.S.E.E. degree from the National Technical University "Kharkov Polytechnic Institute," Kharkov, Ukraine, and the Ph.D. degree in radio communications from Moscow Radio Communications R&D Institute, Moscow, Russia, in 1971. He has held responsible positions in both industry and academia. Currently, he is a Senior Scientist at Rockwell Scientific Company, Thousand Oaks, Calif. He is an author of over 200 publications and 30 inventions. A book *Digital Radio Receivers* (Moscow: Radio & Communications, 1987, in Russian) is among his publications. His current major research interests include communication systems; theory of signals, circuits, and systems; mixed-signal processing; digital signal processing; modulation/demodulation; synchronization; and architecture of digital receivers and transmitters.

Gennady Y. Poberezhskiy received the M.S.E.E. degree (with the highest honors) from Moscow Aviation Institute, Russia, in 1993. He has held systems engineering positions in a number of companies. Currently, he is a Principal Engineer at Raytheon Space and Airborne Systems, El Segundo, Calif. He is an author of 20 publications. His current research interests include communication systems, mixed-signal processing, digital signal processing, communication, and GPS receivers.